Tikrit Journal of Engineering Sciences (2024); 31(4): 158-171
DOI: http://doi.org/10.25130/tjes.31.4.16

IRAQI Academic Scientific Journals

ISSN: 1813-162X (Print); 2312-7589 (Online)
Tikrit Journal of Engineering Sciences
available online at: http://www.tj-es.com

TJES Tikrit Journal of Engineering Sciences

Performance Evaluation of Different NEMA Induction Motor Designs under the Effect of Unbalanced Supply Voltages

Hilmi F. Ameen *, Hayder A. Hamad, Ali A. Rasool
Electrical Engineering Department, Engineering College, Salahadddin University-Erbil, Erbil, Iraq.

Keywords:
Induction Motors (IMs); NEMA Designs; Under voltage Unbalance (UVU); Over Voltage Unbalance (OVU); Voltage Unbalance Factor (VUF).

Highlights:

- *Performance analysis of different NEMA designs of IMs under unbalanced supply voltage.*
- *Investigation of the effect of different unbalanced voltage magnitudes for similar VUF with OVU and UVU on different NEMA designs.*
- *The MATLAB Software used for simulation purpose.*

ARTICLE INFO
Article history:

Received	21 Oct.	2023
Received in revised form	26 Jan.	2024
Accepted	25 Mar.	2024
Final Proofreading	25 Oct.	2024
Available online	30 Dec.	2024

Citation: Ameen HF, Hamad HA, Rasool AA. **Performance Evaluation of Different NEMA Induction Motor Designs under the Effect of Unbalanced Supply Voltages**. *Tikrit Journal of Engineering Sciences* 2024; **31**(4): 158-171.
http://doi.org/10.25130/tjes.31.4.16

**Corresponding author:*

Hilmi F. Ameen
Electrical Engineering Department, Engineering College, Salahadddin University-Erbil, Erbil, Iraq.

Abstract: Three-phase induction motors (IMs) are generally used in commercial, industrial, and domestic applications due to their advantages, such as good self-starting ability, simplicity, high reliability, cost-effectiveness, low maintenance, and ruggedness in construction. The IMs are exposed to different internal and external faults; one of the most popular external faults is unbalanced supply voltages. Unbalanced supply voltage is a popular and worldwide phenomenon that effectively decreases the characteristics of IMs. The present work shows the adverse effect of unbalanced supply voltages on the steady-state characteristics of all NEMA (National Electrical Manufacturers Association) designs of 20hp squirrel cage IMs (SCIMs). A symmetrical component is used to determine the performance of each NEMA design operating in different unbalanced supply voltage situations. The importance of this paper is that it likens different NEMA designs regarding torque-speed characteristics, efficiency, power factor, stator currents, rotor currents, torque pulsation, a ripple in rotor speed, and starting-up performances when subjected to over and under-unbalanced supply voltage conditions. Also, the MATLAB and Simulink environments have been utilized concurrently for simulation purposes.

تقييم أداء تصاميم الجمعية الوطنية لمصنعي الأجهزة الكهربائية لمختلف أنواع المحركات الحثية تحت تأثير الجهد غير المتوازن

حلمي فاضل امين، حيدر احمد حمد، علي عبد القادر رسول
قسم الهندسة الكهربائية/ كلية الهندسة/ جامعة صلاح الدين-أربيل/ أربيل – العراق.

الخلاصة

تُستخدم المحركات الحثية ثلاثية الطور بشكل عام في التطبيقات التجارية والصناعية والمنزلية نظرًا لمزاياها، مثل القابلية الجيدة على البدء الذاتي، والبساطة، والموثوقية العالية، والتكلفة الاقتصادية، وانخفاض الصيانة، والمتانة في التركيب. تتعرض المحركات الحثية لأعطال داخلية وخارجية مختلفة؛ أحد أكثر أنواع الأعطال الخارجية شيوعًا هو الجهد غير المتوازن. يعد الجهد غير المتوازن ظاهرة شائعة وعالمية وقد ثبت أنها فعالة جدًا في تقليل خصائص المحركات الحثية. في هذه الدراسة، يتم عرض التأثير السلبي للجهود غير المتوازنة على خصائص الحالة المستقرة لجميع تصاميم الجمعية الوطنية لمصنعي الاجهزة الكهربائية للمحرك الحثي ذي القفص السنجابي بقدرة ٢٠ حصانا. يتم استخدام المركبات المتماثلة لتحديد أداء كل تصميم من التصاميم التي تعمل في حالات مختلفة من الجهد غير المتوازن. تكمن أهمية هذه الدراسة في أنها تشبه تصميمات الجمعية الوطنية لمصنعي الاجهزة الكهربائية المختلفة فيما يتعلق بخصائص السرعة-العزم، والكفاءة، ومعامل القدرة، وتيارات الجزء الثابت، وتيارات الجزء الدوار، ونبض عزم الدوران، والتذبذب في سرعة الدوار، وأداء بدء التشغيل عند التعرض لظروف جهد غير متوازن زائد أو منخفض، علاوة على ذلك، تم استخدام برامج MATLAB وSimulink بشكل متزامن لأغراض المحاكاة.

الكلمات الدالة: المحركات الحثية، تصاميم الجمعية الوطنية لمصنعي الاجهزة الكهربائية، الجهد غير المتوازن المنخفض، الجهد غير المتوازن الزائد، معامل عدم توازن الجهد.

1.INTRODUCTION

In general, three-phase IMs are used in industry applications due to their good features and high reliability and robustness [1]. IMs, which potentially establish emphasized conditions, under which their performance is unfavorably affected, are seen in numerous applications [2]. In addition to its benefits, the squirrel cage induction motor (SCIM) has a low beginning torque. Using SCIMs in some applications that require high beginning torque has been limited. As a result, by modifying the reactance and resistance of the rotor through the shape of the rotor slots and rotor bars of SCIMs, it is possible to improve the beginning and regular running performance. The NEMA criterion mostly defines four design classes for SCIMs: Design A, design B, design C, and design D [3]. These classes are distinguished by the shape of rotor slots, bar materials, and torque-speed performances. The exact balanced supply voltage can never be maintained due to load variation, and an unbalanced voltage can cause severe troubles, leading to many induction motor's unseasonable failures. Since the last three centuries, many researchers have been interested in studying the effect of an unbalanced supply voltage on three-phase IM performance [4]. Generally, electrical motors are designed to work with balanced and pure sinusoidal supply voltages. Anwari and Hiendro [5], a complete symmetrical component mathematical model for determining the output power of the IM that works under unbalanced voltages, considering corresponding angles and neglecting constant losses, has been proposed. Refs. [6, 7] examined the harmful effects of unbalanced supply voltage on IMs properties. They found that the current unbalance factor (CUF) was 6–10 times higher than the voltage unbalance factor (VUF). The performance of three-phase IMs was simulated using the finite element method under unbalanced supply voltage conditions [8]. A complete investigation of the impact of positive and negative voltage portions, as well as the angle between them, on motor performance is presented [4]. El-Kharashi et al. [9] presented the behavior and efficiency of two dissimilar kinds of IMs coupled and working with balanced and imbalanced supply voltages. The effects of the positive sequence voltage component part on IMs losses, developed torque, and the sensibility of motor variables were investigated by Adekitan [10]. A new definition of phase imbalance index was proposed by [10, 11] for different scenarios by presenting a simple comparison of voltage supply quality in terms of phase angle, which regards the normal 120° displacement of a three-phase supply. The operational data of three-phase IM running subjected to balanced and unbalanced voltage supplies was simulated using data mining [12]. The effects of voltage unbalance and harmonic distortions on different efficiency IM classes behavior were investigated [13, 14]. They deduced that the losses due to voltage unbalance and harmonic distortion of the IM were greater in the IM's higher efficiency classes. A complete mathematical model of static rotor resistance chopper speed control of slipring IMs subjected to the unbalanced supply voltage at different duty cycles was proposed and discussed by [15]. A mathematical model for predicting the behavior of slip energy recovery under unbalanced supply voltage at different inverter firing angles was proposed in [16]. In Refs. [17, 18], a simulation model using MATLAB/Simulink for analyzing the steady state performance of the three-phase IM under different unbalanced supply voltage conditions was proposed. The performance of a three-phase induction motor subjected to the operation of single-phasing effects in steady-state conditions under different supply voltage

unbalances is presented in [19]. A regular analysis of the effects of voltage unbalance and harmonic distortion on the drive systems of IMs was presented by [20]. It was found that the voltage unbalance significantly affected the developed torque compared to the harmonic effects. The non-sinusoidal supply voltage impact on the steady-state characteristics of NEMA designs of SCIMs related to the skin effect was investigated in [21]. Donolo et al. [22] concluded that vibrations caused by voltage imbalance were notably more prominent in larger efficiency IMs than the standard efficiency IMs. The literature reports many studies on decreasing losses and increasing the efficiency of IMs regarding voltage unbalance. For example, improving the IM efficiency can be attained by modifying the stator and rotor design and their parameters, simultaneously considering the quality of the supply voltage. Based on the previous discussion, the present paper investigates the steady-state characteristics of NEMA designs A, design B, design C, and design D of SCIMs under the effect of an unbalanced supply voltage. The symmetrical component technique and mathematical equations related to the IMs equivalent model are presented. Furthermore, this paper studies the effect of different unbalanced voltage magnitudes for similar VUF with OVU and UVU on the developed electromagnetic torque, stator current, rotor current, torque pulsation, speed fluctuation, power factor, and efficiency. The remaining sections of the paper are as follows: Section two discusses the research method and modeling of SCIM under an unbalanced supply voltage. Section three presents the results and discussion, and the last section is the conclusion.

2.THE RESEARCH METHODOLOGY

In typical electrical power distribution system analysis, a balanced state is assumed. Voltage unbalance is a voltage disturbance in the positive sequence induced by the negative and zero-sequence voltage components. The zero-sequence component is zero since the IMs are connected in mesh or wye connections without neutrality. Therefore, voltage imbalance is mainly caused by the negative sequence components [23]; correspondingly, the voltage imbalance is the emplacement of negative sequence voltage over positive sequence voltage. Whenever the positive sequence voltage component is disrupted, and its value gets smaller than the rated value, this phenomenon is under voltage. In contrast, for more than the rated value, the state is overrated voltage. The steady-state analysis of 3-phase IMs operating under an unbalanced supply voltage is traditionally conveyed by applying the symmetrical component technique, using the positive and negative sequence equivalent models of IMs. Figure 1 displays the per-phase equivalent circuit of designs A, B, and D of IMs.

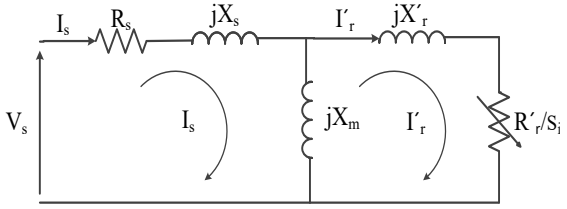

Fig. 1 Per-Phase Equivalent Circuit for Designs A, B, and D.

Where V_s is the applied motor phase voltage, I_s is the stator phase current, R_s and X_s are stator resistance and reactance per phase, respectively, I_r is the rotor referred current, R'_r and X'_r are the referred rotor resistance and reactance, respectively, and X_m is the magnetizing reactance. The input impedance for the positive sequence model and the negative sequence impedance may be determined from Fig. 1, where i = 1 for the positive sequence and i = 2 for the negative sequence. The operating slip (s_1):

$$s_1 = \frac{n_s - n}{n_s} \quad (1)$$

Where ns is the synchronous speed of Ims, and n is the rotor speed. The negative sequence slip (s_2):

$$s_2 = 2 - s_1 \quad (2)$$

The input impedance:

$$Z_{inp} = R_S + jX_s + \frac{(jX_m)\left(\frac{R'_r}{s_i} + jX'_r\right)}{\frac{R'_r}{s_i} + j(X_m + X'_r)} \quad (3)$$

Using the method of mesh analysis, the matrix equations obtained are:

$$\begin{bmatrix} V_s \\ 0 \end{bmatrix} = \begin{bmatrix} Z_s + Z_o & -Z_0 \\ -Z_0 Z_0 + Z'_r \end{bmatrix} \begin{bmatrix} I_s \\ I'_r \end{bmatrix} \quad (4)$$

where $Z_s = R_s + jX_s$, $Z_0 = jX_0$, *and* $Z'_r = \frac{R'_r}{s_i} + jX'_r$:

Inverting Eq. (4) to determine the stator and rotor currents:

$$\begin{bmatrix} I_s \\ I'_r \end{bmatrix} = \frac{V_s}{Z_s Z'_r + Z_o(Z_s + Z'_r)} \begin{bmatrix} Z_0 + Z'_r \\ Z_0 \end{bmatrix} \quad (5)$$

Determining the motor performance requires the positive and negative sequences of stator and rotor currents, which can be calculated by the Fortescue matrix transformation, as shown in Eqs. (6) – (9):

$$\begin{bmatrix} V_{sp} \\ V_{sn} \end{bmatrix} = \frac{1}{3} \begin{bmatrix} 1 & a & a^2 \\ 1 & a^2 & a \end{bmatrix} \begin{bmatrix} V_{sa} \\ V_{sb} \\ V_{sc} \end{bmatrix} \quad (6)$$

where a=exp(j2π/3) is the Fortescue operator, and the voltage unbalance factor (VUF) defined by the IEC [23, 24] is:

$$VUF = \left|\frac{V_{sn}}{V_{sp}}\right| \times 100 \quad (7)$$

$$\begin{bmatrix} I_{sp} \\ I_{sn} \end{bmatrix} = \frac{1}{3} \begin{bmatrix} 1 & a & a^2 \\ 1 & a^2 & a \end{bmatrix} \begin{bmatrix} I_{sa} \\ I_{sb} \\ I_{sc} \end{bmatrix} \quad (8)$$

$$\begin{bmatrix} I_{rp} \\ I_{rn} \end{bmatrix} = \frac{1}{3}\begin{bmatrix} 1 & a & a^2 \\ 1 & a^2 & a \end{bmatrix}\begin{bmatrix} I_{ra} \\ I_{rb} \\ I_{rc} \end{bmatrix} \quad (9)$$

The stator current unbalance factor (CUFs) and rotor current unbalance factor (CUF_r) are given by Eqs. (10), (11):

$$CUF_s = \left|\frac{I_{sn}}{I_{sp}}\right| \quad (10)$$

$$CUF_r = \left|\frac{I_{rn}}{I_{rp}}\right| \quad (11)$$

The total input of active and reactive power into the motor is given by:

$$P_{in} = Re\left[3 * \left(V_{sp}I_{sp}^{*} + V_{sn}I_{sn}^{*}\right)\right] \quad (12)$$

$$Q_{in} = Im\left[3 * \left(V_{sp}I_{sp}^{'*} + V_{sn}I_{sn}^{'*}\right)\right] \quad (13)$$

The input power factor can be determined with:

$$pf = \cos\left[tan^{-1}\left(\frac{Q_{in}}{P_{in}}\right)\right] \quad (14)$$

The negative sequence portion of an unbalanced supply voltage develops an air-gap rotating magnetic field against the direction of the rotor, producing an undesirable negative sequence component. As a result, torque pulsation, speed reduction, more losses, and motor derating occur. Furthermore, because of the negative sequence circuit's low impedance value, a high negative sequence current increases motor loss and decreases motor life. The electromagnetic torque, developed by the IMs under an unbalanced supply voltage, is the resultant torque developed by the positive sequence component and negative sequence component of the rotor currents, which is given by:

$$T_e = T_p + T_n = 3\frac{R'_r}{\omega_s}\left(\frac{I_{rp}^2}{s_1} - \frac{I_{rn}^2}{s_2}\right) \quad (15)$$

The motor efficiency can be given by:

$$\eta = \frac{P_{out}}{P_{in}} \times 100 \quad (16)$$

The performance analysis of design C (double cage IM) can be investigated depending on the equivalent circuit, as shown in Fig. 2.

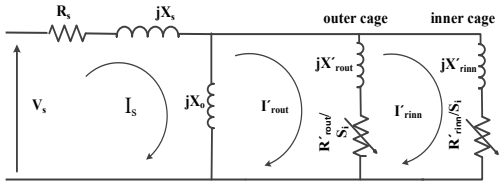

Fig. 2 Per-Phase Equivalent Circuit for Design C (Double Cage).

The mesh equation for this model is:

$$\begin{bmatrix} V_s \\ 0 \\ 0 \end{bmatrix} = \begin{bmatrix} Z_s + Z_o & -Z_0 & 0 \\ -Z_0 Z_0 + Z'_{rout} & -Z'_{rout} & \\ 0 & -Z'_{rout} Z'_{rout} + Z'_{rinn} & \end{bmatrix}\begin{bmatrix} I_s \\ I'_{rout} \\ I'_{rinn} \end{bmatrix} \quad (17)$$

where $Z'_{rout} = \frac{R'_{rout}}{S_i} + j\,X'_{rout}$ and $Z'_{rinn} = \frac{R'_{rinn}}{S_i} + j\,X'_{rinn}$.

The determent of Eq. (17) is given by:

$$\Delta = (Z_s + Z_0(Z_0 + Z'_{rout})(Z'_{rout} + Z'_{rinn}) - (Z_s + Z_0)Z'^{2}_{rout} - (Z'_{rout} + Z'_{rinn})Z_0^{2} \quad (18)$$

The stator current can be calculated from:

$$\begin{bmatrix} I_s \\ I'_{rout} \\ I'_{rinn} \end{bmatrix} = V_s\begin{bmatrix} Y_{11} \\ Y_{21} \\ Y_{31} \end{bmatrix} \quad (19)$$

Where:

$$Y_{11} = \frac{1}{\Delta}\begin{bmatrix} Z_0 + Z'_{rout} & -Z'_{rout} \\ -Z'_{rout} & Z'_{rout} + Z'_{rinn} \end{bmatrix} \quad (20)$$

$$Y_{21} = \frac{-1}{\Delta}\begin{bmatrix} -Z_0 & 0 \\ -Z'_{rout} & Z'_{rout} + Z'_{rinn} \end{bmatrix} \quad (21)$$

$$Y_{31} = \frac{1}{\Delta}\begin{bmatrix} -Z_0 & 0 \\ Z_0 + Z'_{rout} & -Z'_{rout} \end{bmatrix} \quad (22)$$

The input power and the power factor can be calculated from Eqs. (12) - (14). The electromagnetic torque developed by the IM under unbalanced supply voltage conditions is the resultant torque developed by the positive sequence component and negative sequence component of the outer cage rotor current and inner cage rotor current, which is given by Eq.(23):

$$T_e = (T_{Pout} + T_{Pinn}) - (T_{nout} + T_{ninn}) = \frac{3}{\omega_s}\left[\begin{array}{l} \left(\frac{(I'_{rpout})^2 R'_{rout}}{s_1} + \frac{(I'_{rpinn})^2 R'_{rinn}}{s_1}\right) \\ -\left(\frac{(I'_{rnout})^2 R'_{rout}}{s_2} + \frac{(I'_{rninn})^2 R'_{rinn}}{s_2}\right) \end{array}\right] \quad (23)$$

The impact of an unbalanced supply voltage on the electromagnetic torque developed can be analyzed using the torque ripple factor (TRF) and can be calculated from:

$$TRF\% = \frac{Te_{pp}}{Te_{ave}} \times 100 \quad (24)$$

where Te_{pp} and Te_{ave} are peak-to-peak and average developed torque, respectively.

3.RESULTS AND DISCUSSION

The harmful impact of the unbalanced supply voltage on the characteristics of NEMA design A, design B, design C, and design D with the same rating of wye-connected, 20 hp, 400 V, 50 Hz, two-poles were examined, and the parameters are given in Table 1. The four designs IMs were examined with unbalanced supply voltage as a function of VUF, which is allowed to vary between (0-7) % to exceed the NEMA recommended limit (5%) for over and under voltage supply, as shown in Table 2, to investigate which designs have been mainly affected. Phase A was adjusted to $231\angle 0^0$, and the two remaining phases, B and C, were adapted to obtain the required VUF% by changing the value and the angle of phase C and comparing with the same VUF for UVU and OVU conditions. The MATLAB/Simulink, as shown in Fig. 3, is implemented to examine the performance of different NEMA design models under different unbalanced voltage levels, such as the electromagnetic torque response, the rotor speed response, ripple in speed, and torque pulsation.

Table 1 The Motor Parameters of All NEMA Designs [25].

Design	A	B	C	D
RS(Ω)	0.1456	0.1456	0.1456	0.1456
Rr/(Ω)	0.3267	0.46961	0.684 (inn. cage) 2.521 (out. cage)	1.36
XS(Ω)	0.7681	0.7681	0.7681	0.7681
Xr/(Ω	0.7681	1.1772	1.822 (inn. cage) 0.582 (out. cage)	0.7681
Xm(Ω)	33.3	33.3	33.5	33.3

Table 2 The Supply Voltages, Positive Sequence Supply Voltage Component, Negative Sequence Supply Voltage Component, and VUF% Supplied to Each NEMA Design.

VUF%	Case	Va(V)	Vb(V)	Vc(V)	Vp(V)	Vn(V)
0	Bal.	$231\angle 0^0$	$231\angle -120^0$	$231\angle 120^0$	$231\angle 0^0$	0
1	UVU	$231\angle 0^0$	$228.84\angle -120.88^0$	$226.8\angle 120^0$	$228.81\angle -0.29^0$	$2.32\angle 29.8^0$
3		$231\angle 0^0$	$225\angle -122.84^0$	$218.9\angle 120^0$	$224.91\angle -0.88^0$	$6.88\angle 30^0$
5		$231\angle 0^0$	$221.84\angle -124.5^0$	$211.6\angle 120^0$	$221.3\angle -1.44^0$	$11.11\angle 30^0$
7		$231\angle 0^0$	$218.55\angle -126^0$	$204\angle 120^0$	$217.48\angle -2^0$	$15.33\angle 30^0$
1	OVU	$231\angle 0^0$	$233\angle -119.1^0$	$235.05\angle 120^0$	$233.1\angle 0.31^0$	$2.37\angle -149.8$
3		$231\angle 0^0$	$236.88\angle -117.4^0$	$243.6\angle 120^0$	$237.1\angle 0.86^0$	$7.22\angle -148.2^0$
5		$231\angle 0^0$	$240.5\angle -115.7^0$	$251.8\angle 120^0$	$240.9\angle 1.43^0$	$12.03\angle -147.5^0$
7		$231\angle 0^0$	$245\angle -114^0$	$256.2\angle 120^0$	$243.6\angle -2.34^0$	$17.2\angle -149.5^0$

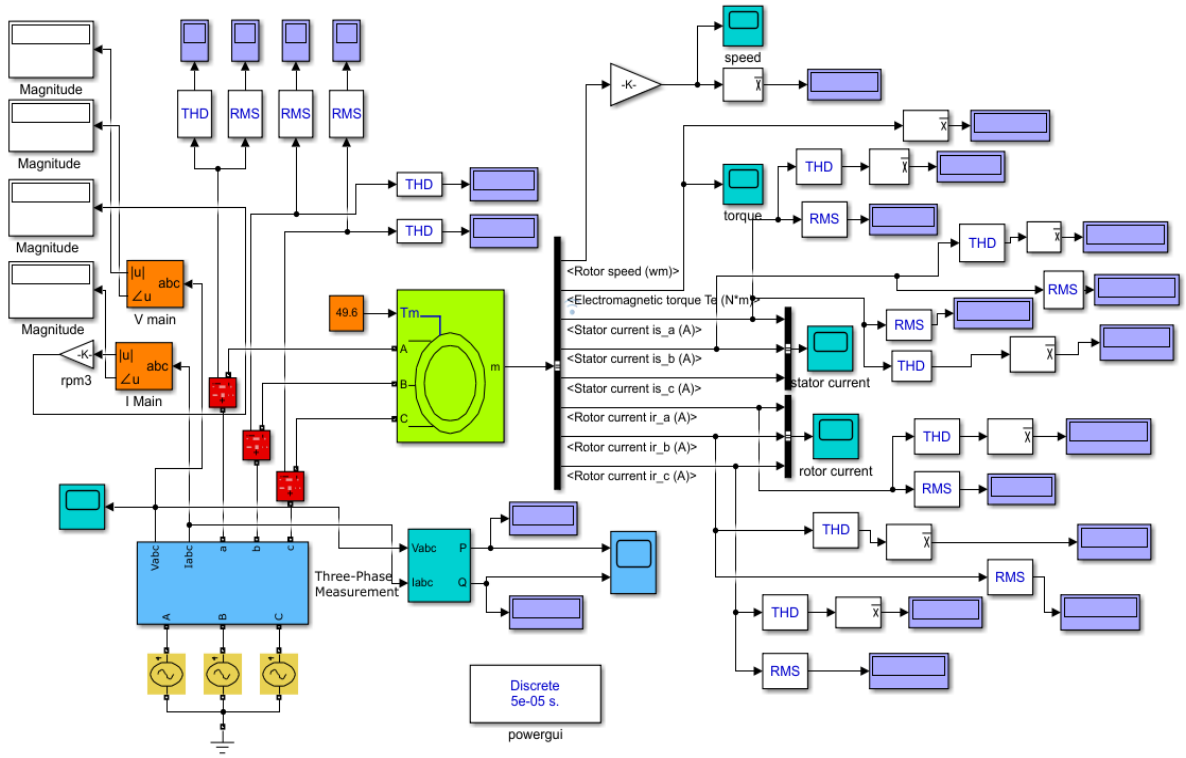

Fig. 3 The SIMULINK Model of Three-Phase IM under Different Unbalanced Supply Voltage.

3.1.The Effect of Unbalanced Supply Voltage on the Torque-Speed Characteristics

The torque-speed characteristics for all NEMA design IMs under different unbalanced supply voltage conditions are shown in Fig. 4, which shows the change of electromagnetic torque developed with motor speed in various values of VUF from (0-7) % in the range of UVU and OVU. It can be noted that with decreasing VUF from (7% of OVU) to (7% of UVU) the rotor speed decreases. Table 3 displays the motor speed, starting torque, and pull-out torque variation for each NEMA design at full load under varying voltage unbalance conditions. It can be seen that with increasing the VUF for OVU, the rotor speed increased by 12 rpm (design A), 19 rpm (design B), 20 rpm (design C), and 49 rpm (design D), while the rotor speed decreased with UVU by 14 rpm (design A), 22 rpm (design B), 28 rpm (design C), and 66 rpm (design D). Design D was more affected than the other designs. Furthermore, in the same table, it can be noted that the increasing or decreasing of starting torque with UVU and OVU was more affected by this phenomenon in design D, whereas the starting torque increased by (17.3 Nm) for OVU and decreased by (16.6 Nm) with UVU in design D, while for design B it increased by (6.54 Nm with OVU) and

decreased by (6.26 Nm with UVU). In addition, it can be shown that the increasing or decreasing of maximum torque with UVU and OVU in designs A and B was more affected by VUF, whereas the maximum torque increased by 18.2 Nm for OVU and decreased by 16.4 Nm with UVU in design A, while for design B it increased by (14.3 Nm with OVU) and decreased by (12.9 Nm with UVU). Table 4 shows the simulation response results for design A, design B, design C, and design D for settling time (Ts) and rising time (Tr) with VUF% for different voltage-unbalanced conditions. It should be noticed that for all designs with increasing VUF, the Ts and Tr were reduced for OVU, and increased for UVU voltage-unbalanced conditions. The simulation response results for design A, design B, design C, and design D are observed in Table 4 for settling time (Ts) and rising time (Tr) with VUF% for different voltage unbalance conditions. It should be noticed that for all designs with increasing VUF, the Ts and Tr were reduced for OVU, and increased for UVU voltage unbalance conditions. Further research revealed that NEMA design B had the lowest torque pulsation and rotor speed ripples, whereas NEMA design C had the fewest Ts and Tr. Figure 5 shows the linear characteristics between torque ratio factor TRF% and VUF for OVU and UVU supply voltage conditions. It can be seen that design A and design C had the larger TRF% and torque pulsation than design D and design B. On the other hand, Fig. 6 shows the rotor speed ripple versus VUF% for different NEMA designs. It is shown that design A had a maximum speed ripple at VUF of 7% and a minimum at balanced supply voltage. In addition, it can be determined that the effect of OVU on the torque pulsation and rotor speed ripple for the same VUF% was greater than UVU voltage conditions.

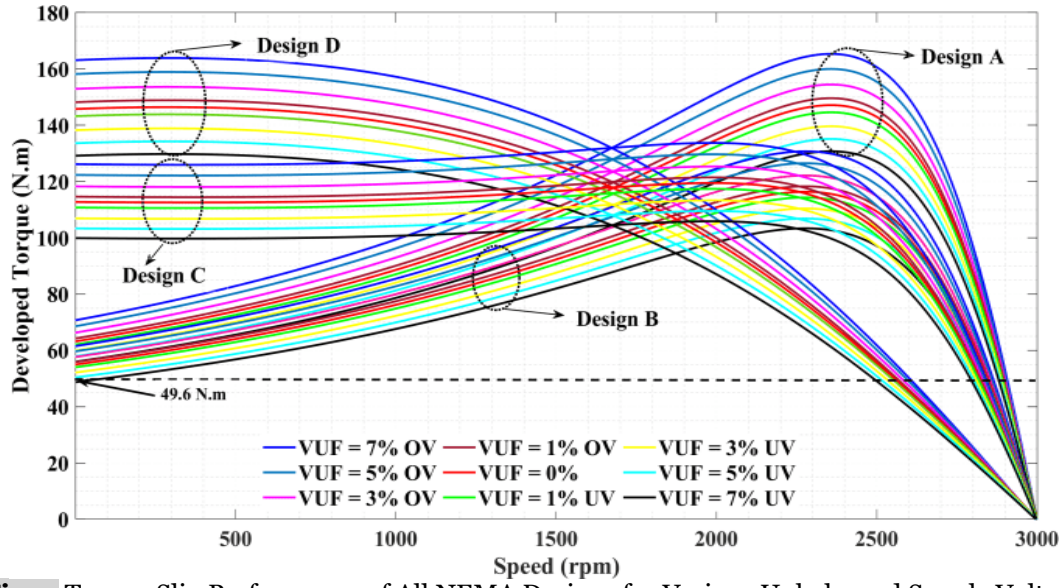

Fig. 4 Torque Slip Performance of All NEMA Designs for Various Unbalanced Supply Voltage Conditions.

Table 3 The Variations of Motor Speed, Starting Torque, and Pull-Out Torque Against VUF% for Various NEMA Designs.

VUF%	Case	Rotor Speed (rpm)				Starting Torque (Nm)				Pull-out Torque (Nm)			
		Design A	Design B	Design C	Design D	Design A	Design B	Design C	Design D	Design A	Design B	Design C	Design D
7	OVU	2906	2868	2841	2606	70.7	61.5	126.1	163.1	165.3	130.7	133.7	163.9
5		2903	2860	2837	2598	68.7	59.7	122.3	158.2	160	126.5	129.7	158.9
3		2900	2853	2831	2581	66.3	57.7	118.2	152.9	154.4	122.1	125.3	153.6
1		2896	2848	2825	2566	64.2	55.9	114.6	148.2	149.6	118.3	121.4	148.8
0		2894	2845	2821	2559	63.2	55	112.7	145.8	147.1	116.3	119.4	146.4
1	UVU	2892	2842	2816	2553	62.2	54.02	110.7	143.2	144.6	114.3	117.4	143.9
3		2888	2838	2810	2536	60	52.17	106.9	138.3	139.6	110.4	113.3	138.8
5		2884	2834	2802	2516	58.0	50.44	103.3	233.7	135.1	106.8	109.5	134.2
7		2880	2829	2793	2493	56	48.74	99.88	129.2	130.7	103.4	105.8	129.7

Table 4 The Change of Settling and Rising Times for Various NEMA Designs as a Function of VUF%.

		Over Voltage				Balance	Under Voltage			
	VUF%	7	5	3	1	0	1	3	5	7
Design A	Ts(msec)	603	645	680	748	845	896	935	1038	1200
	Tr(msec)	276	296	311	328	340	361	387	413	430
Design B	Ts(msec)	780	875	931	1016	1110	1240	1430	1681	2200
	Tr(msec)	350	370	395	424	440	465	515	562	610
Design C	Ts(msec)	320	331	345	375	400	421	428	448	480
	Tr(msec)	207	221	232	246	253	264	270	279	290
Design D	T_s(msec)	421	436	460	486	500	519	538	576	610
	T_r(msec)	215	223	231	235	240	250	266	282	295

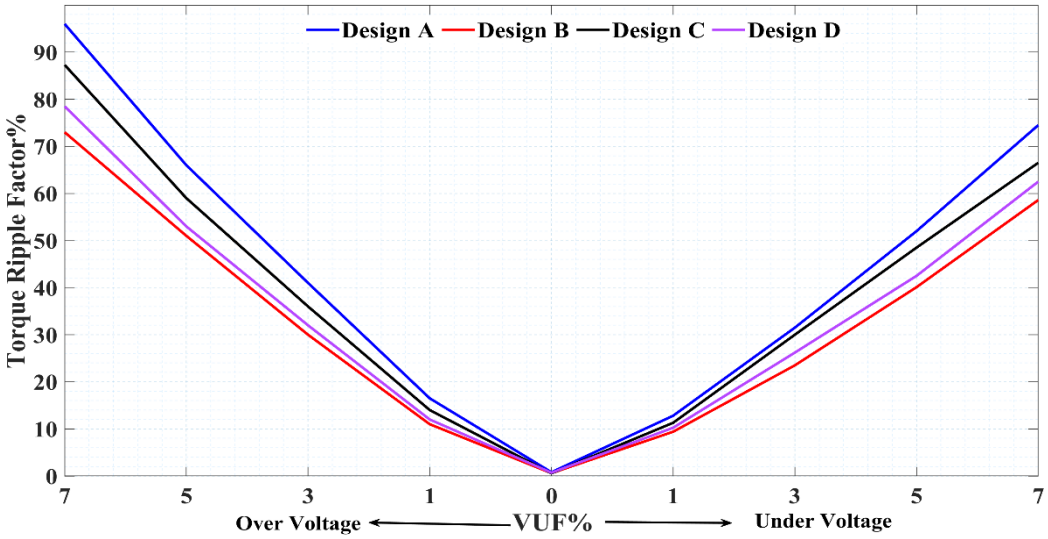

Fig. 5 TRF Against VUF for all NEMA Designs for Various Unbalanced Supply Voltage.

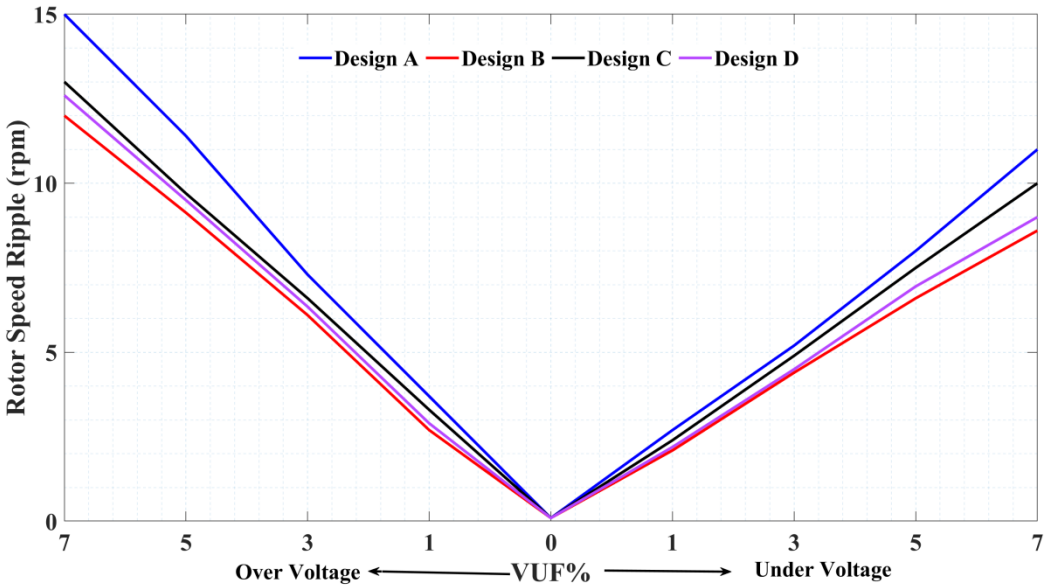

Fig. 6 Rotor Speed Ripple Against VUF for all NEMA Designs for Various Unbalanced Supply Voltage Conditions.

Figures 7, 8, and 9 show the electromagnetic torque developed response at balanced supply voltage (VUF = 0%), under-voltage supply (VUF = 7%), and over-voltage supply (VUF = 7%) for all NEMA designs of IMs, respectively. It can be seen that the time required to reach the steady-state full load torque in design B was greater than in the other three designs due to a high electrical time constant because the ratio of rotor inductance to rotor resistance was higher than in designs A, C, and D, for the same mechanical time constant. At the same time, it was less effective in designs C and D, and the torque pulsation increased with VUF. Overvoltage unbalance caused more torque pulsation than undervoltage unbalance, as shown in Fig. 5. Figures 10, 11, and 12 show the rotor speed response at balanced supply voltage (VUF = 0%), under voltage supply (VUF = 7%), and over-voltage supply (VUF = 7%) for all NEMA design IMs, respectively. It can be seen that the time needed to attain the steady-state

full load speed in design B was greater than in the other three NEMA designs. The rotor speed ripple at the balance supply was about 0.1 rpm for all NEMA designs. However, with increasing VUF, the rotor speed ripple increased in different proportions to about 12 rpm for UVU and to 15 rpm for OVU for design A, as shown in Fig. 5.

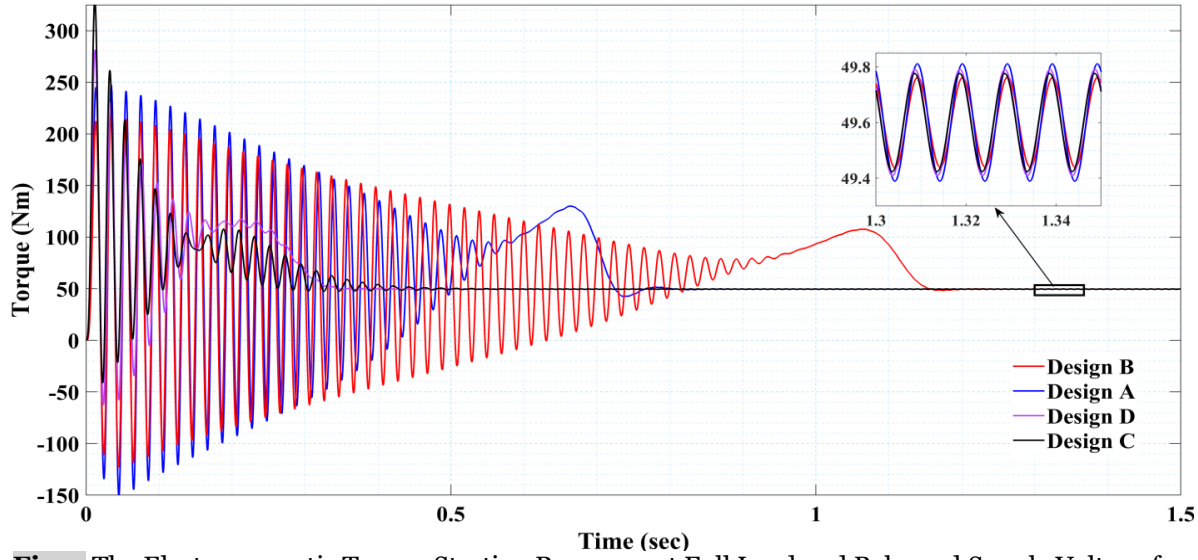

Fig. 7 The Electromagnetic Torque Starting Response at Full Load and Balanced Supply Voltage for different NEMA Design Ims.

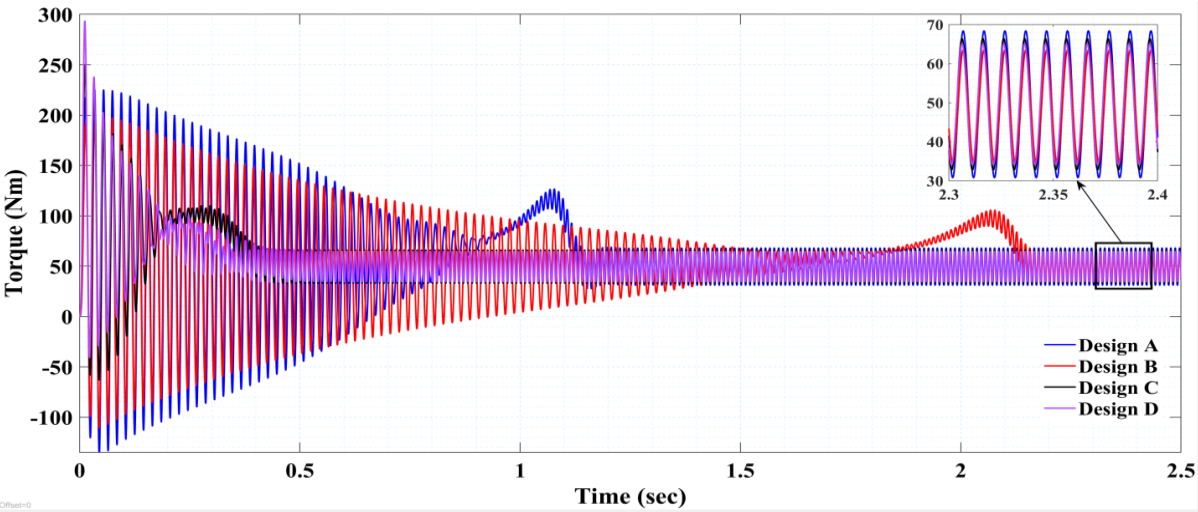

Fig. 8 The Electromagnetic Torque Starting Response at Full Load and under Voltage Unbalance UVU) Supply (VUF=7%) for different NEMA Design Ims.

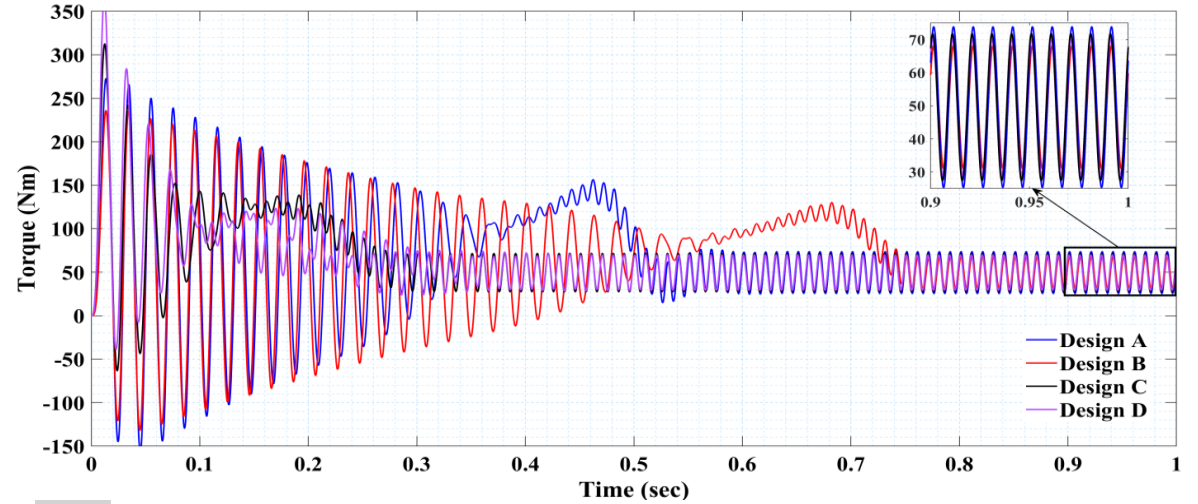

Fig. 9 The Electromagnetic Torque Starting Response at Full Load and Over Voltage Unbalance (OVU) Supply (VUF=7%) for different NEMA Design Ims.

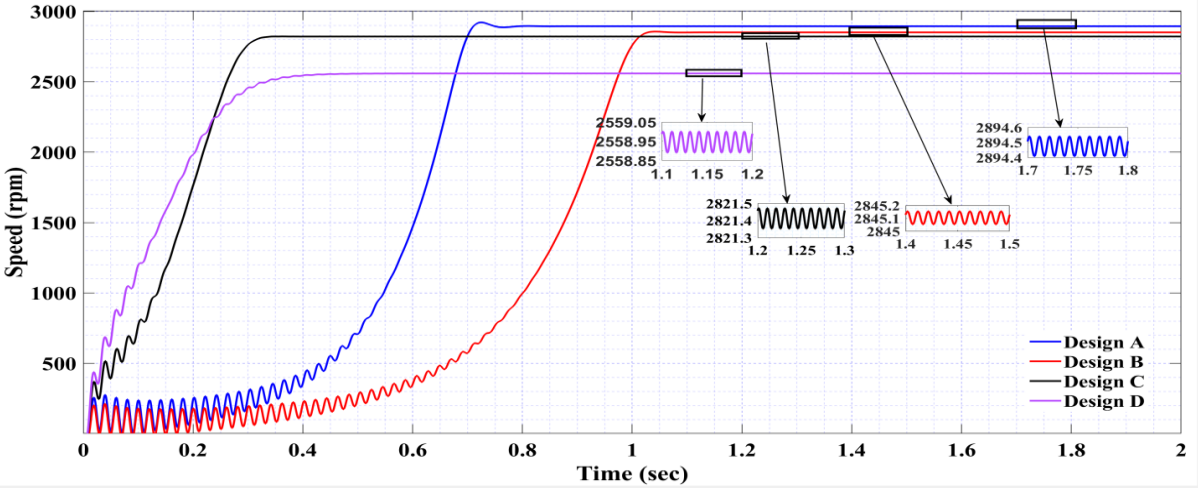

Fig. 10 The Rotor Speed Response at Full Load and Balanced Supply Voltage for different NEMA Design Ims.

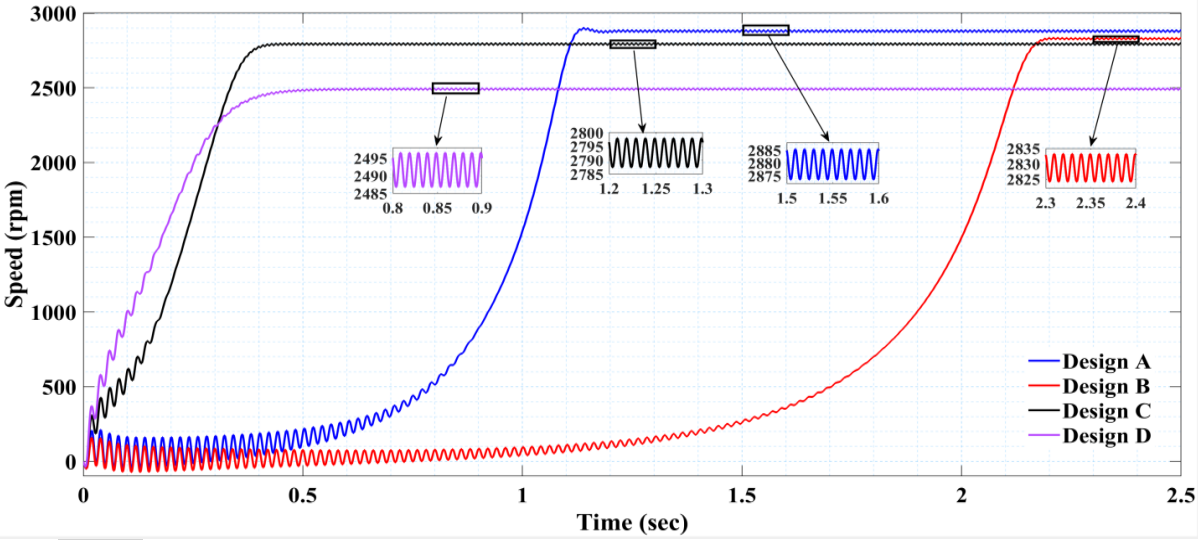

Fig. 11 The Rotor Speed Response at Full Load and under Voltage Unbalance (UVU) Supply (VUF=7%) for different NEMA Design Ims.

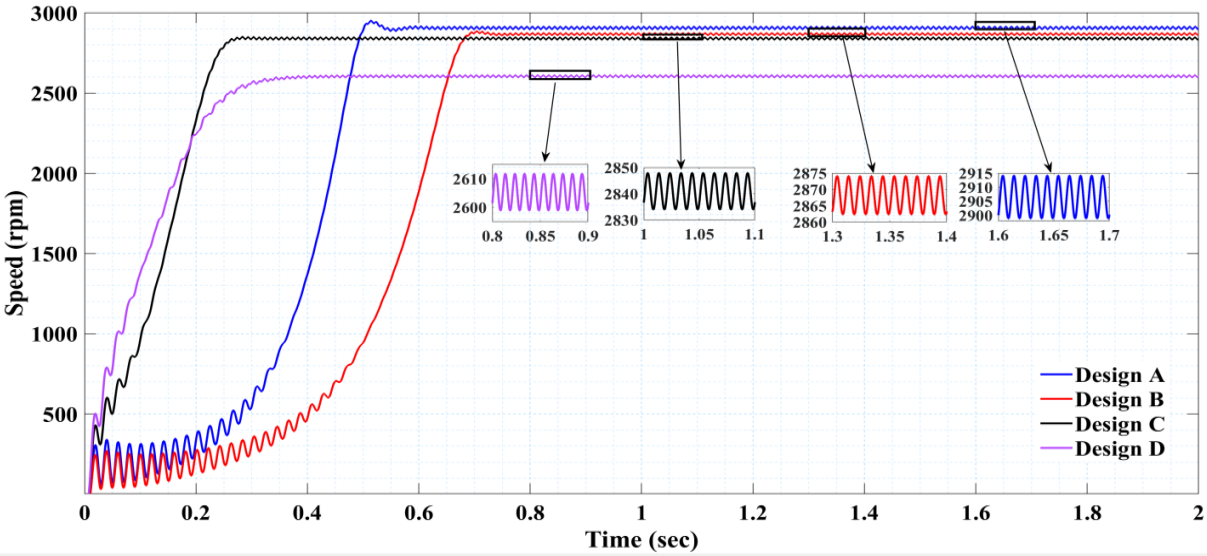

Fig. 12 The Rotor Speed Response at Full Load and Over Voltage Unbalance (OVU) Supply (VUF=7%) for different NEMA Design Ims.

3.2.The Effect of Supply Voltage Unbalance on the Stator and Rotor Currents

The positive-sequence component, negative-sequence component, and CUF for stator and rotor phase currents are given in Figs. 13 and 14, respectively. It is shown that the stator negative-sequence component current for design A increased from (0-12.1) A for OVU and (0-10.05) A for UVU. In contrast, the stator positive-sequence component current decreased from (27.5 to 26) A for OVU and increased from (27.5 to 29.1) A with UVU for design A. It can be noted that the rotor negative-sequence component current for design A increased from (0-11.62) A for OVU and (0-9.68) A for UVU, whereas the rotor positive-sequence current decreased from (26.12 to 24.53) A for OVU and from (26.12 to 27.83) A for UVU. The CUF of the stator for design A, which was the largest, varied from 45.8% (OVU) to 33.1% (UVU). Besides, design B, which had the minimum variation, varied from 35.1% (OVU) to 25.7% (UVU). The CUF of rotor current for design A, which was the largest, varied from 47.3% (OVU) to 34.8% (UVU). Besides, design B, which had the minimum variation, varied from 36.65% (OVU) to 26.68% (UVU). It can be concluded that the CUF of stator and rotor currents of NEMA design A had a larger value than design B, which had a lower value in OVU and UVU supply voltage conditions. Figure 15 displays the positive and negative sequence impedance change against VUF for UVU and OVU for different NEMA designs. It can be noted that all positive sequence impedances slightly decreased (for OVU) or increased (for UVU) with changing VUF, while the negative sequence impedance fell notably with VUF.

3.3.The Effect of Supply Voltage Unbalance on Power Factor and Efficiency

The variation of different NEMA design power factors against VUF for OVU and UVU unbalanced supply voltage conditions is shown in Fig. 16. It is clear that by increasing the VUF in the OVU and UVU regions, the power factor decreased. It is observed that the power factor slightly increased for VUF (0–3) % in UVU due to decreasing phase B and phase C voltages and then its magnetizing current, while for OVU, it still decreased because of increasing the magnetizing current due to increasing phase B and phase C phase voltages. Further, the power factor of designs A and B was less than that of designs C and D. Figure 17 presents the motor efficiency versus VUF for UVU and OVU. As the asymmetry of the supply voltage increased for OVU and UVU, the efficiency decreased. The efficiency decreased with increasing voltage unbalance, especially in the OVU region, because the negative sequence current (copper losses) effect was greater than the power factor increase rate. As a result, efficiency decreased. It can be noted that the efficiency of all NEMA designs decreased with the VUF for OVU more than with the same VUF for UVU. The efficiency of design A at zero VUF was 89.5%, and when VUF% was 7 (OVU), it was 87.5%. Meanwhile, with the same VUF%, the efficiency was 88.3% with UVU.

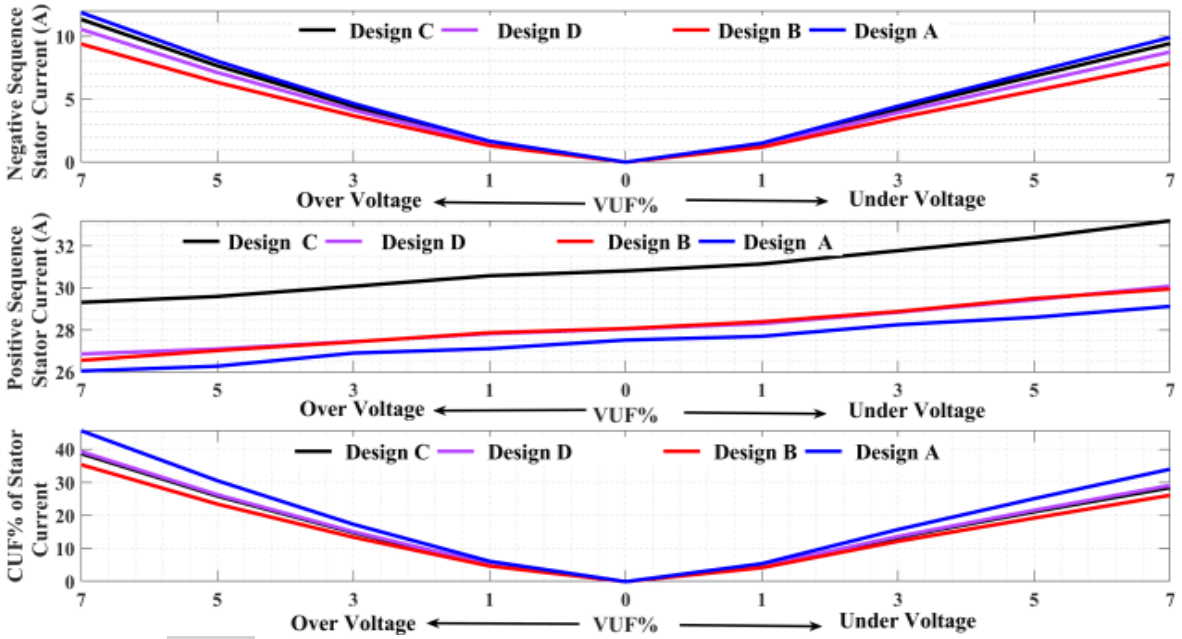

Fig. 13 Negative, Positive, and CUF% of Stator Currents Against VUF%.

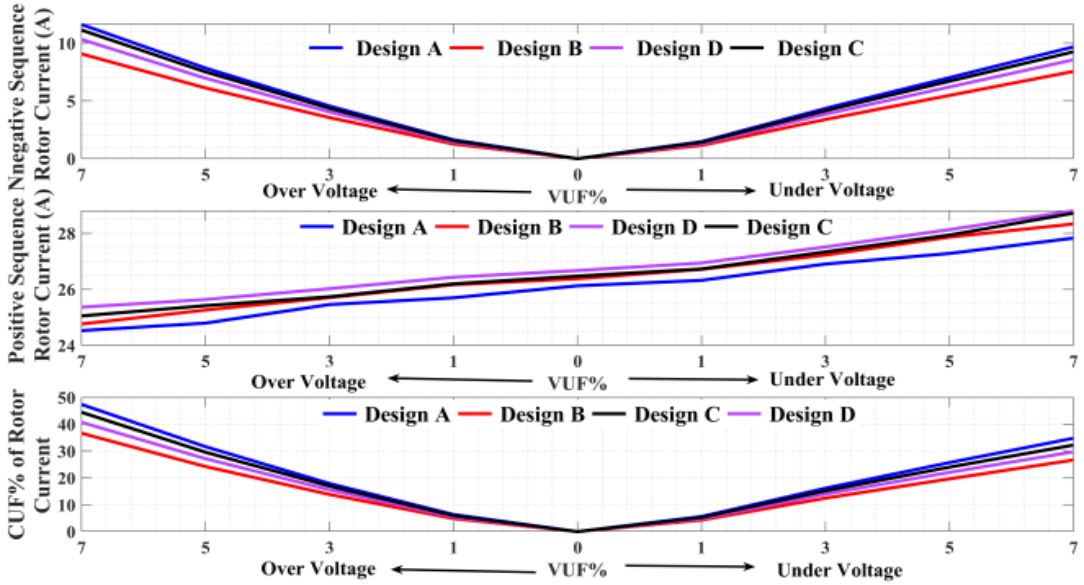

Fig. 14 Negative, Positive, and CUF% of Rotor Currents Against VUF%.

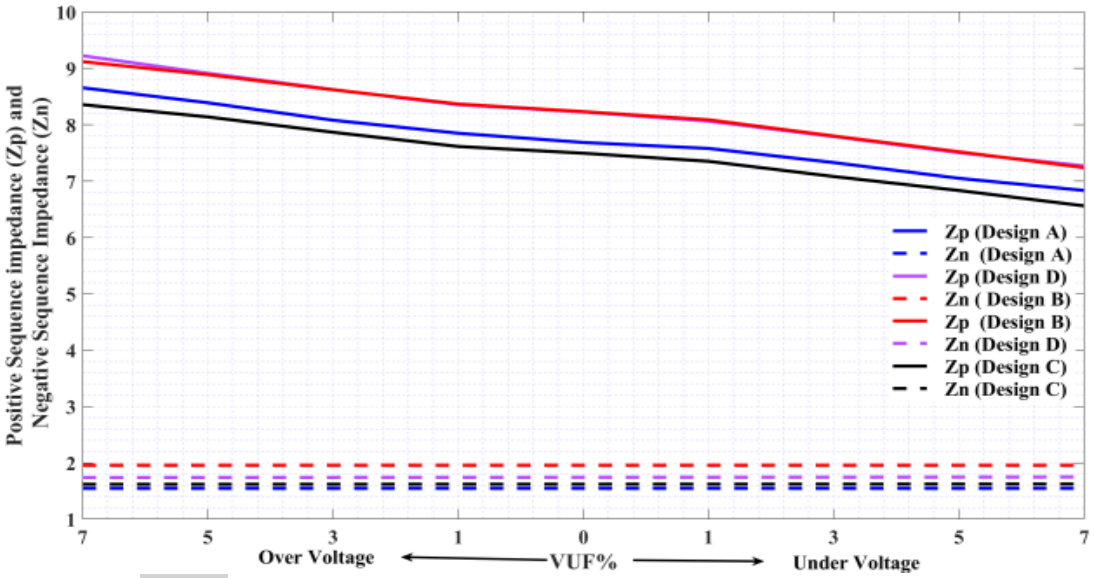

Fig. 15 The Positive and Negative Sequence Impedances Versus VUF% for different NEMA Designs.

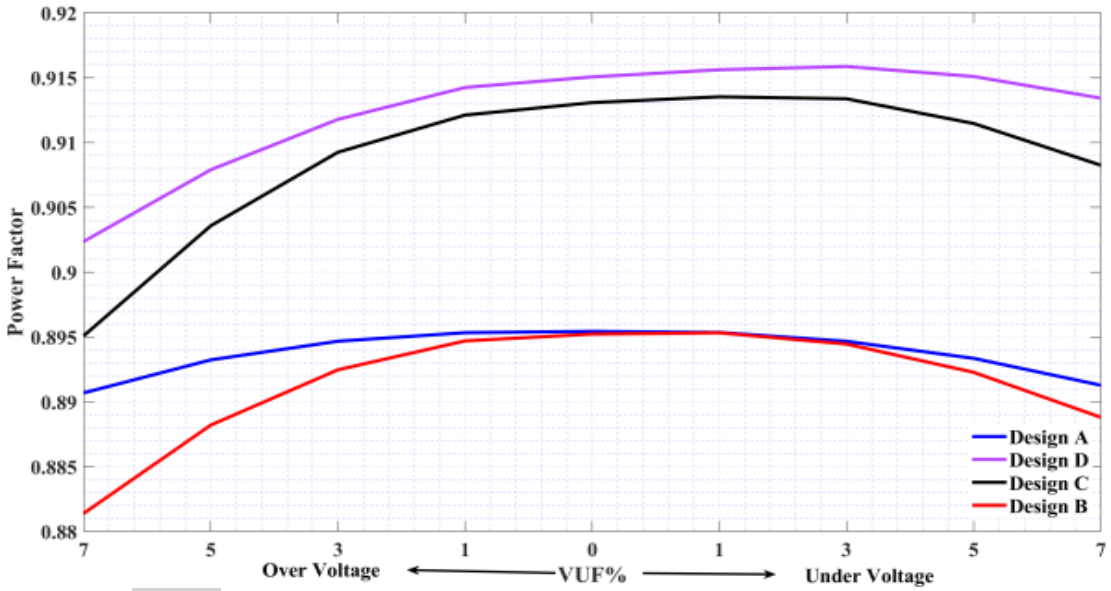

Fig. 16 The Power Factor Variation with VUF for different NEMA Designs.

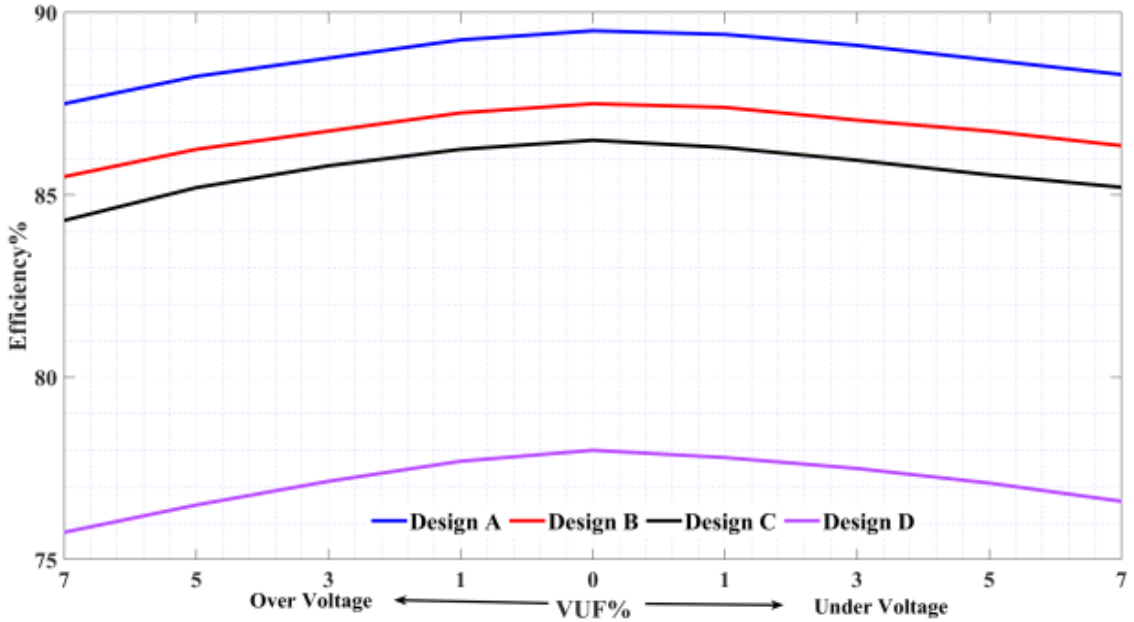

Fig. 17 The Variation of Efficiency with VUF for different NEMA Designs.

4.CONCLUSION

Globally, reducing energy waste due to voltage unbalance will help save some millions of dollars paid out annually on unusable energy wasted largely as heat. This paper analyses the steady-state performance for different NEMA designs of IMs under the impact of unbalanced supply voltage combined with over-voltage and under-voltage unbalance conditions. It can be seen that the sensitivity of all NEMA designs of IMs to unbalanced supply voltage is different according to the obtained results. The following conclusions can be drawn based on the present paper:

1) The positive and negative equivalent circuit models were presented, and their effects on the net torque-speed characteristics were described. The negative sequence portion of torque decreased the starting torque, pull-out torque, and speed at the rated load. The NEMA design D of IM had larger starting and pull-out torque than other designs.

2) The startup time in case of under-unbalanced supply voltage conditions was larger than over-voltage unbalanced supply conditions. In contrast, the torque pulsation and rotor speed ripple in case of over-voltage unbalance was more than under voltage unbalanced conditions for all NEMA designs of IM.

3) The rotor speed ripple and torque pulsation values increased with VUF under unbalanced supply voltage conditions. It can be noted that NEMA design A had the maximum deviation in ripples for rotor speed (15 rpm) and percentage torque ripple factor (95%), while NEMA design B had a smaller variation in rotor speed variation (12 rpm) and percentage ripple factor of 72% than other designs.

4) For the same VUF, the power factor dropped with increasing positive sequence voltage (OVU) rather than the negative sequence voltage component due to stator magnetic core saturation, decreasing magnetizing reactance, and increasing magnetizing current. As a result, more reactive power was drawn.

5) Positive and negative sequence voltage components affected motor efficiency. In design A, the efficiency decreased (from 89.5 % to 8.5%) with increasing the VUF (0-7)%, and it decreased from 89.5% to 88.2% under voltage-unbalanced supply conditions.

REFERENCES

[1] Jassim AH, Hussein AA, Abbas LF. **The Performance of a Three-Phase Induction Motor under and Over Unbalance Voltage**. *Tikrit Journal of Engineering Sciences* 2021; **28**(2):15-32.

[2] Adouni A, Cardoso JM. **Thermal Analysis of Low-power Three-Phase Induction Motors Operating under Voltage Unbalance and Inter-Turn Short Circuit Faults**. *Machines* 2020; **9**(2): 1-11.

[3] Lee HJ, Im SH, Um DY, Park GS. **A Design of Rotor Bar for Improving Starting Torque by Analyzing Rotor Resistance and Reactance in Squirrel Cage Induction Motor**. *IEEE Transactions on Magnetics* 2017; **54**(3): 1-4.

[4] Quispe EC, López ID, Ferreira FJ, Sousa SV. **Unbalanced Voltages Impacts on**

the Energy Performance of Induction Motors. *International Journal of Electrical and Computer Engineering* 2018; **8**(3): 1412-1422.

[5] Anwari M, Hiendro A. **New Unbalance Factor for Estimating Performance of a Three-Phase Induction Motor with under and Overvoltage Unbalance**. *IEEE Transactions on Energy Conversion* 2010;**25**(3):619-625.

[6] Youb L. **Effects of Unbalanced Voltage on the Steady State of the Induction Motors**. *International Journal of Electrical Energy* 2014; **2**(1): 34-38.

[7] Patil RU, Chaudari HB. **Behavior of Induction Motor at Voltage Unbalanced**. *International Journal of Engineering Research & Technology* 2015; **4**(5): 1344-1348.

[8] Ebadi A, Mirzaie M, Gholamian SA. **Investigation of the Effects of Unbalanced Voltages on the Performance of a Three-Phase Squirrel Cage Induction Motor Using Finite Element Method**. *Majlesi Journal of Electrical Engineering* 2013; **7**(2): 76-82.

[9] El-Kharashi E, Massoud JG, Al-Ahmar MA. **The Impact of the Unbalance in Both the Voltage and the Frequency on the Performance of Single and Cascaded Induction Motors**. *Energy* 2019; **181**: 561-575.

[10] Adekitan AI. **A New Definition of Voltage Unbalance Using Supply Phase Shift**. *Journal of Control, Automation and Electrical Systems* 2020; **31**(3): 718-725.

[11] Singh S, Srivastava A. **Voltage Unbalance and Its Impact on the Performance of Three Phase Induction Motor: A Review**. *International Journal for Research in Applied Science & Engineering Technology* 2019;**7**(7): 106-111.

[12] Adekitan AI, Adewale A, Olaitan A. **Determining the Operational Status of a Three Phase Induction Motor Using a Predictive Data Mining Model**. *International Journal of Power Electronics and Drive System* 2019;**10**(1): 93-103.

[13] Donolo PD, Pezzani CM, Bossio GR, De Angelo CH, Donolo MA. **Derating of Induction Motors Due to Power Quality Issues Considering the Motor Efficiency Class**. *IEEE Transactions on Industry Applications* 2020; **56**(2):961-969.

[14] Tabora J M, De Matos E, Soares TM, Tostes ME. **Voltage Unbalance Effect on the Behavior of IE2, IE3 and IE4 Induction Motor Classes**. *Simpósio Brasileiro de Sistemas Elétricos-SBSE* 2020; **1**(1): 1-6.

[15] Ameen HF, Aula FT. **Performance Analysis and Modeling of SRRCCIM under the Impact of Unbalance Supply Voltage**. *Journal of Electrical and Electronics Engineering* 2021; **14**(1): 5-10.

[16] Ameen HF, Aula FT. **Performance Analysis of the Slip Power Recovery Induction Motor Drive System under Unbalance Supply Voltages**. *Advances in Electrical and Electronic Engineering* 2021;**19**(3): 192-202.

[17] Martínez AB, Navarro IJ, Santos VS, Quispe EC, Donolo PD. **MATLAB/Simulink Modeling of Electric Motors Operating with Harmonics and Unbalance**. *International Journal of Electrical and Computer Engineering* 2022; **12**: 4640-4648.

[18] Jasim AH, Jasim TZ. **Dynamic Performance Analysis of Three Phase Induction Motor Using Matlab/Simulink Technique**. *Tikrit Journal of Engineering Sciences* 2015; **22**(2): 117-130.

[19] Abbas LF, Ahmed RE, Mahmmoud ON, Gaeid KS, Mokhlis HB. **Single Phasing Effects on the Behavior of Three-Phase Induction Motor**. *Tikrit Journal of Engineering Sciences* 2023; **30**(4): 11-18.

[20] Beleiu HG, Pavel SG, Birou IM, Miron A, Darab PC, Sallah M. **Effects of Voltage Unbalance and Harmonics on Drive Systems with Induction Motor**. *Journal of Taibah University for Science* 2022; **16**(1): 381-391.

[21] Othman NA, Ameen HF. **The Influence of Non-Sinusoidal Voltage Sources on the Stea dy State Performance of Different NEMA Designs of IMs**. *Zanco Journal of Pure and Applied Sciences* 2022; **34**(6): 8-19.

[22] Donolo PD, Pezzani C, Bossio GR, De Angelo CD, Donolo M. **Vibration Magnitude Analysis on Induction Motors of Different Efficiency Classes Due to Voltage Unbalance**. *IEEE Transactions on Industry Applications* 2023; **59**(3): 2913-2918.

[23] Wang YJ. **Analysis of Effects of Three-Phase Voltage Unbalance on Induction Motors with Emphasis on the Angle of the Complex Voltage Unbalance Factor**. *IEEE Transactions on Energy Conversion* 2001; **16**(3): 270-275.

[24] Faiz J, Ebrahimpour H, Pillay P. **Influence of Unbalanced Voltage on**

the Steady-State Performance of a Three-Phase Squirrel-Cage Induction Motor. *IEEE Transactions on Energy Conversion* 2004; **19**(4): 657-662.

[25] Pedra J, Sainz L, Córcoles, F. **Harmonic Modeling of Induction Motors**. *Electric Power Systems Research* 2006; **76**(11): 936-944.